

8-22-2015

Multi-Sampling Ionization Chamber (MUSIC) for measurements of fusion reactions with radioactive beams

P. F.F. Carnelli
Argonne National Laboratory

S. Almaraz-Calderon
Argonne National Laboratory

K. E. Rehm
Argonne National Laboratory

M. Albers
Argonne National Laboratory

M. Alcorta
Argonne National Laboratory

See next page for additional authors

Follow this and additional works at: https://repository.lsu.edu/physics_astronomy_pubs

Recommended Citation

Carnelli, P., Almaraz-Calderon, S., Rehm, K., Albers, M., Alcorta, M., Bertone, P., Digiovine, B., Esbensen, H., Fernández Niello, J., Henderson, D., Jiang, C., Lai, J., Marley, S., Nusair, O., Palchan-Hazan, T., Pardo, R., Paul, M., & Ugalde, C. (2015). Multi-Sampling Ionization Chamber (MUSIC) for measurements of fusion reactions with radioactive beams. *Nuclear Instruments and Methods in Physics Research, Section A: Accelerators, Spectrometers, Detectors and Associated Equipment*, 799, 197-202. <https://doi.org/10.1016/j.nima.2015.07.030>

This Article is brought to you for free and open access by the Department of Physics & Astronomy at LSU Scholarly Repository. It has been accepted for inclusion in Faculty Publications by an authorized administrator of LSU Scholarly Repository. For more information, please contact ir@lsu.edu.

Authors

P. F.F. Carnelli, S. Almaraz-Calderon, K. E. Rehm, M. Albers, M. Alcorta, P. F. Bertone, B. Digiovine, H. Esbensen, J. Fernández Niello, D. Henderson, C. L. Jiang, J. Lai, S. T. Marley, O. Nusair, T. Palchan-Hazan, R. C. Pardo, M. Paul, and C. Ugalde

1 **A Multi-Sampling Ionization Chamber (MUSIC) for Measurements**
2 **of Fusion Reactions with Radioactive Beams**

3 P.F.F. Carnelli^{a,b,c}, S. Almaraz-Calderon^{a,1}, K.E. Rehm^{a,*}, M. Albers^{a,2}, M.
4 Alcorta^{a,3}, P.F. Bertone^{a,4}, B. Digiovine^a, H. Esbensen^a, J. Fernández Niello^{b,d}, D.
5 Henderson^a, C.L. Jiang^a, J. Lai^e, S.T. Marley^{a,5}, O. Nusair^a, T. Palchan-Hazan^a,
6 R.C. Pardo^a, M. Paul^f, and C. Ugalde^a

7 ^a*Physics Division, Argonne National Laboratory, Argonne, Illinois 60439, USA*

8 ^b*Laboratorio TANDAR, Comisión Nacional de Energía Atómica, Av. Gral. Paz 1499,*
9 *B1650KNA, San Martín, Buenos Aires, Argentina*

10 ^c*Consejo Nacional de Investigaciones Científicas y Técnicas, Av. Rivadavia 1917, C1033AAJ,*
11 *Buenos Aires, Argentina*

12 ^d*Universidad Nacional de San Martín, Campus Miguelete, B1650BWA, San Martín, Buenos*
13 *Aires, Argentina*

14 ^e*Department of Physics and Astronomy, Louisiana State University, Baton Rouge, Louisiana*
15 *70803, USA*

16 ^f*Racah Institute of Physics, Hebrew University, Jerusalem, Israel*

17 *Corresponding author Tel.: +1 (630) 252-4073, Fax: +1 (630) 252-6210, e-mail: rehm@anl.gov

18 PACS: 25.60.Pj, 29.40.Cs; 26.30.Ca; 29.38.Gj

19 *Keywords:* Active Target Detector; Multi-Sampling Ionization Chamber; Fusion Reactions

20
21 **Abstract**

¹ Present address: Department of Physics, Florida State University, Tallahassee, Florida 32306, USA.

² Present address: Ernst & Young GmbH, 65760 Eschborn, Germany.

³ Present address: TRIUMF, Vancouver, British Columbia VGT 2A3, Canada.

⁴ Present address: Marshall Space Flight Center, Huntsville, Alabama 35812, USA.

⁵ Present address: Department of Physics, University of Notre Dame, Notre Dame, Indiana 46556, USA.

22 A detection technique for high-efficiency measurements of fusion reactions with low-intensity radioactive
23 beams was developed. The technique is based on a Multi-Sampling Ionization Chamber (MUSIC)
24 operating as an active target and detection system, where the ionization gas acts as both target and
25 counting gas. In this way, we can sample an excitation function in an energy range determined by the gas
26 pressure, without changing the beam energy. The detector provides internal normalization to the incident
27 beam and drastically reduces the measuring time. In a first experiment we tested the performance of the
28 technique by measuring the $^{10,13,15}\text{C}+^{12}\text{C}$ fusion reactions at energies around the Coulomb barrier.

29

30 1. Introduction

31 Fusion reactions play an important role in nature, starting from the creation of the light elements in the
32 Big Bang. They are crucial for the production of heavier elements in the stars' quiescent burning phase as
33 well as in stellar explosions. Fusion processes also generate the energy in the Sun that created and
34 maintains life as we know it. In nuclear physics, fusion reactions can produce exotic nuclei away from
35 stability on the proton-rich side of the mass valley and they are crucial for the production of very heavy
36 nuclei. The availability of radioactive beams at first-generation facilities over the last 20 years has opened
37 many new possibilities for the study of fusion reactions. Particularly, for nuclear structure studies
38 reactions with unstable nuclei offer the possibility to reach even further away from the valley of stability.

39 Fusion between carbon isotopes has attracted the attention of physicists and astronomers for the last 50
40 years. From fundamental nuclear structure effects to recent discoveries in stellar phenomena, there are
41 still many open questions. One of them is the presence of oscillations in the $^{12}\text{C}+^{12}\text{C}$ fusion cross sections
42 that are not observed in neighboring systems and are not completely understood yet [1]. In nuclear
43 astrophysics, fusion reactions involving neutron-rich carbon isotopes may play a fundamental role
44 opening new paths for nucleosynthesis in x-ray binaries, where new explosive phenomena called
45 superbursts have recently been observed [2].

46 In most cases, fusion reactions in the laboratory are studied via the identification of the evaporation
47 residues (ERs) using a variety of experimental techniques. The identification of the ERs can be achieved
48 by detecting the decay radiation from characteristic energy levels or by direct particle detection. For the
49 first case, γ - (e.g., Refs. [3-5]), β - (e.g., Ref. [6]), or x-ray measurements (e.g., Refs. [7-9]) are frequently
50 employed. For the second case, the ERs can be directly detected in $\Delta E-E_{\text{res}}$ detector telescopes mounted
51 at small scattering angles. For that, thin Si ΔE detectors or ionization chambers have been used (see, for
52 example, Refs. [1, 10]). Time-of-flight (ToF) techniques, i.e. measuring the velocities and the energy of
53 the ERs, or gas-filled separators [11] have also been employed in the past.

54 By using one of these methods, excitation functions are obtained by varying the energy of the beam and
55 using large high-efficiency detector arrays (in the decay radiation case), or measuring angular
56 distributions of the ERs (in direct measurements). These experiments require a good relative
57 normalization between the measurements made at different energies. For experiments with low-intensity
58 radioactive beams the measurements can be very time consuming since typically only one cross section is
59 obtained at each bombarding energy.

60 As an alternative, a Multi-Sampling Ionization Chamber (MUSIC) is presented here. The MUSIC is a
61 small gas-filled detector which operates at low beam intensities ($\sim 10^4$ particles/s), counting both incident
62 particles and reaction products. It is also capable of measuring several energy points of an excitation
63 function at once. The detector operates as an active target, i.e. the ionization gas serves as target for the
64 reaction and as detection medium at the same time. The projectile loses energy along its path inside the
65 detector and fusion occurs with different energies depending on the position inside the detector. Since an
66 ER is heavier than a beam particle, it will suffer a significantly larger energy loss. Therefore, the detected
67 energy loss ΔE will suddenly increase at the position where a fusion reaction occurred and the ER will
68 stop inside the detector, which is the signature of a fusion event.

69 Multi-sampling detectors have been employed in the past for the study of heavy-ion reactions. A multi-
70 sampling ionization chamber was first developed for measurements with relativistic heavy ions [12].
71 Later multi-sampling proportional counters [13, 14] were built for experiments with relativistic as well as
72 with low-energy heavy ions. All these detectors, however, are generally quite large (typically 1 m long)
73 which can lead to complications when isotopically enriched gases are to be used as an active target.

74 This paper is organized as follows: in Sect. 2 we give details of the main design features and the
75 operational principle of the MUSIC detector. In Sect. 3 we describe the experimental setup for using the
76 detector at the ATLAS facility at Argonne National Laboratory and the general procedure for its
77 operation, whereas the performance of the technique under real experimental conditions is given in Sect.
78 4. A summary and future perspectives are presented in Sect. 5.

79

80 **2. Schematic and operational principle**

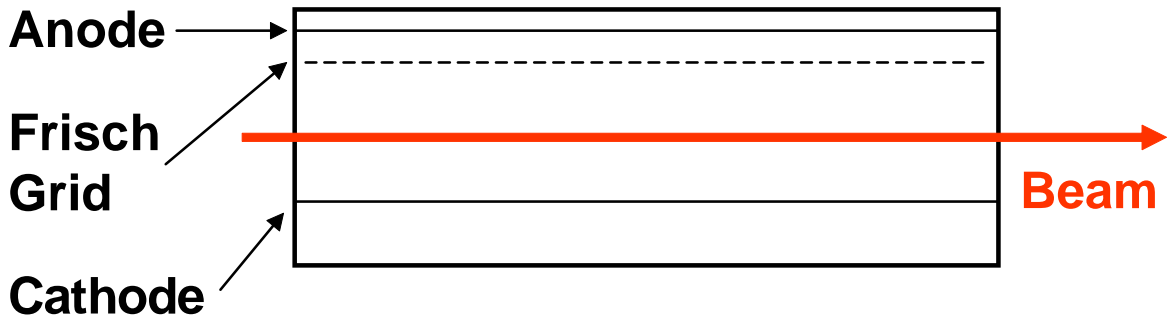
81 The schematic of the multi-sampling ionization chamber MUSIC is shown in Fig. 1. The ionization
82 chamber is mounted inside a 30 cm (L) \times 10 cm (W) \times 20 cm (H) aluminum box that can be filled with a
83 suitable counting gas (He, CH₄, Ne, Ar). In the following we discuss as an example the fusion reactions
84 between $^{10,13,15}\text{C}$ and ^{12}C studied by detecting the evaporation residues in MUSIC, which was filled with
85 CH₄ at 200 mbar thus providing the ^{12}C target. The beams, $^{10,13,15}\text{C}$, were obtained from the heavy ion
86 accelerator ATLAS. Beams of the stable ^{13}C were accelerated in a tandem Van de Graaff accelerator,
87 while beams of radioactive $^{10,15}\text{C}$, with half-lives of 19.3 s and 2.46 s, respectively, were obtained via the
88 in-flight method [15]. The beam production technique is discussed in Sect. 3.3 and more details can be
89 found in Ref. [15]. The $^{10,13,15}\text{C}$ beams enter and exit the detector through 1.45 mg/cm² thick titanium
90 windows. Titanium was chosen to minimize the production of ERs in the window material. In this
91 experiment we have used non-enriched methane (CH₄) gas as active target, for its good counting
92 properties and because reactions with the hydrogen do not interfere with the events of interest at the
93 energies studied in this experiment. The correction for the 1% contamination from ^{13}C was in all cases
94 smaller than the statistical uncertainty of the measured fusion cross sections.

95 In order to obtain the multi-sampling capabilities of the MUSIC detector, the anode of the ionization
96 chamber is segmented in a pattern shown in the lower part of Fig. 1. There are a total of 18 strips
97 numbered from 0 to 17, with each strip being 1.58 cm long. The “active strips” are numbered from 1 to
98 16, while the first and last strips, S_0 and S_{17} , serve as so-called “control strips”. While the segmentation

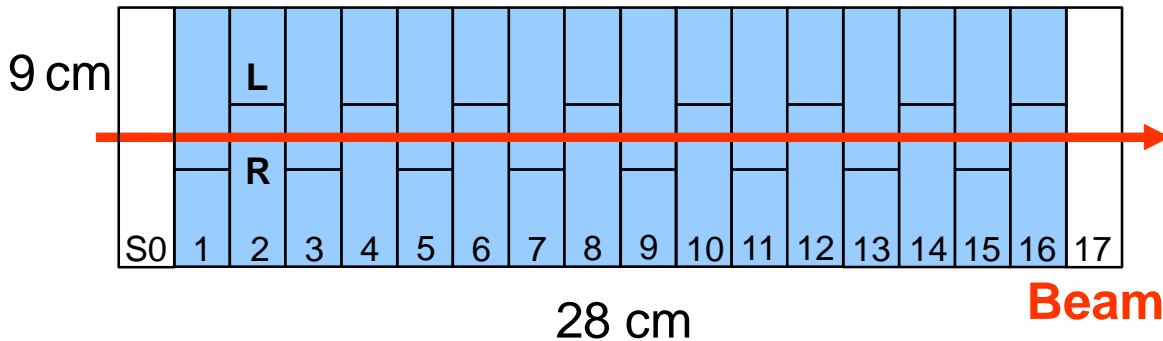
99 chosen for this detector does not allow a full tracking of the individual particles, it allows a clean
 100 identification of fusion events as well as the elimination of elastic and inelastic scattering events based on
 101 their multiplicity. This will be discussed below.

102 The energy signals from the anode were read out using Mesytec MPR-16 preamplifiers and Mesytec
 103 MSCF-16 shaper amplifiers [16]. In addition there were four more energy signals from the control strips
 104 S_0 and S_{17} , from the Frisch grid and from the cathode of the ionization chamber that were read out with
 105 standard NIM electronics.

MUSIC



Schematic of the anode structure



106

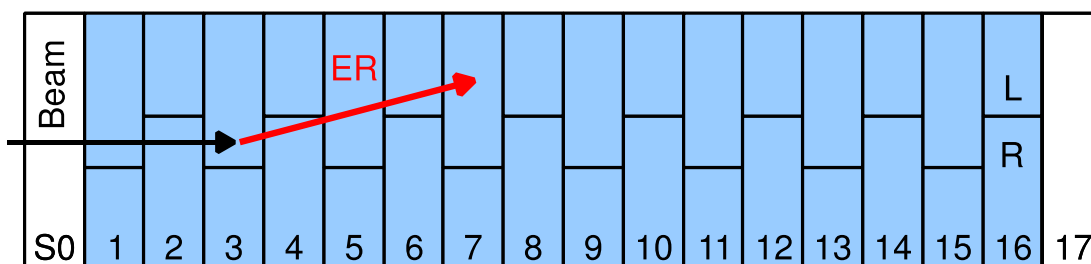
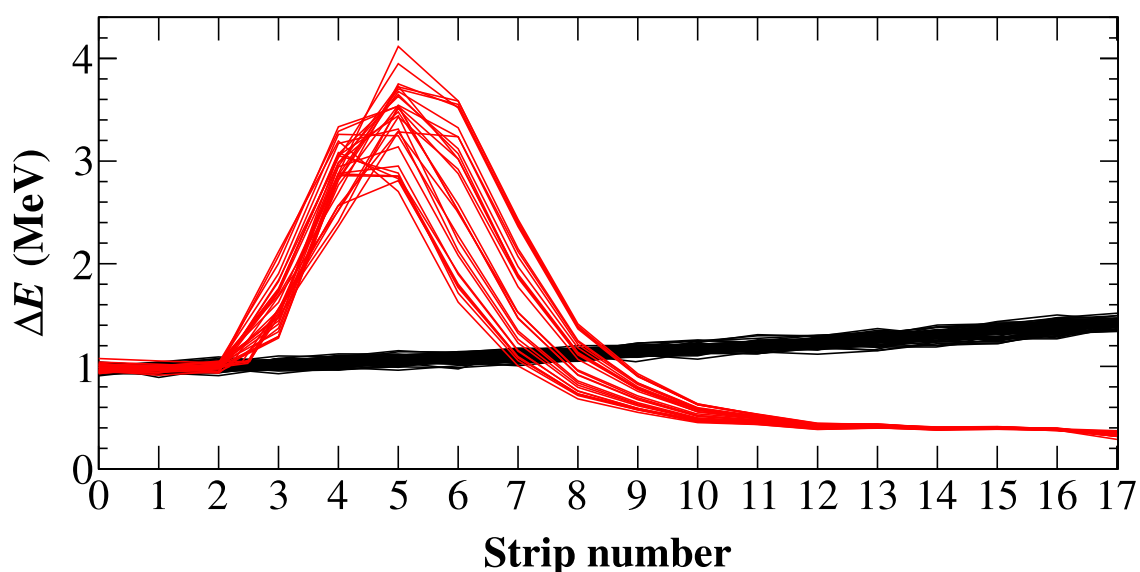
107 Fig. 1 (color online). Schematic of the Multi-Sampling Ionization Chamber (MUSIC). In the upper panel there is a
 108 lateral view of the detector and in the lower panel the structure of the anode.

109 The information provided by the MUSIC detector for a single incoming particle is best represented in a
 110 plot of ΔE vs. *strip number*, which is called a “trace”. As an example, Fig. 2 shows some experimental
 111 traces measured for the $^{13}\text{C}+^{12}\text{C}$ system with a ^{13}C beam at $E_{\text{lab}} = 45$ MeV. The beam reaches the first
 112 active strip (S_1) with an energy of 39 MeV and loses a total of 19 MeV in the active volume of gas
 113 providing the signals $S_1 - S_{16}$. Thus, at this beam energy and gas pressure (200 mbar), the excitation

114 function of $^{13}\text{C}+^{12}\text{C}$ fusion is being sampled in the c.m. energy range of 10-18 MeV in 16 steps of about
 115 0.5 MeV each. If it does not undergo a nuclear reaction, the ^{13}C beam deposits on average about 1.2 MeV
 116 in each strip and, hence, a signal of a beam particle passing through the MUSIC consists of 18
 117 consecutive signals of 1.0 to 1.4 MeV each, as can be seen by the black lines in Fig. 2.

118 A fusion reaction occurring e.g. in strip 3 (see red lines in Fig. 2) starts as beam-like ^{13}C signals followed
 119 by a sudden increase in ΔE (caused by the higher nuclear charge and mass of the ER), and finishes with
 120 no signals because the ER is stopped inside the detector.

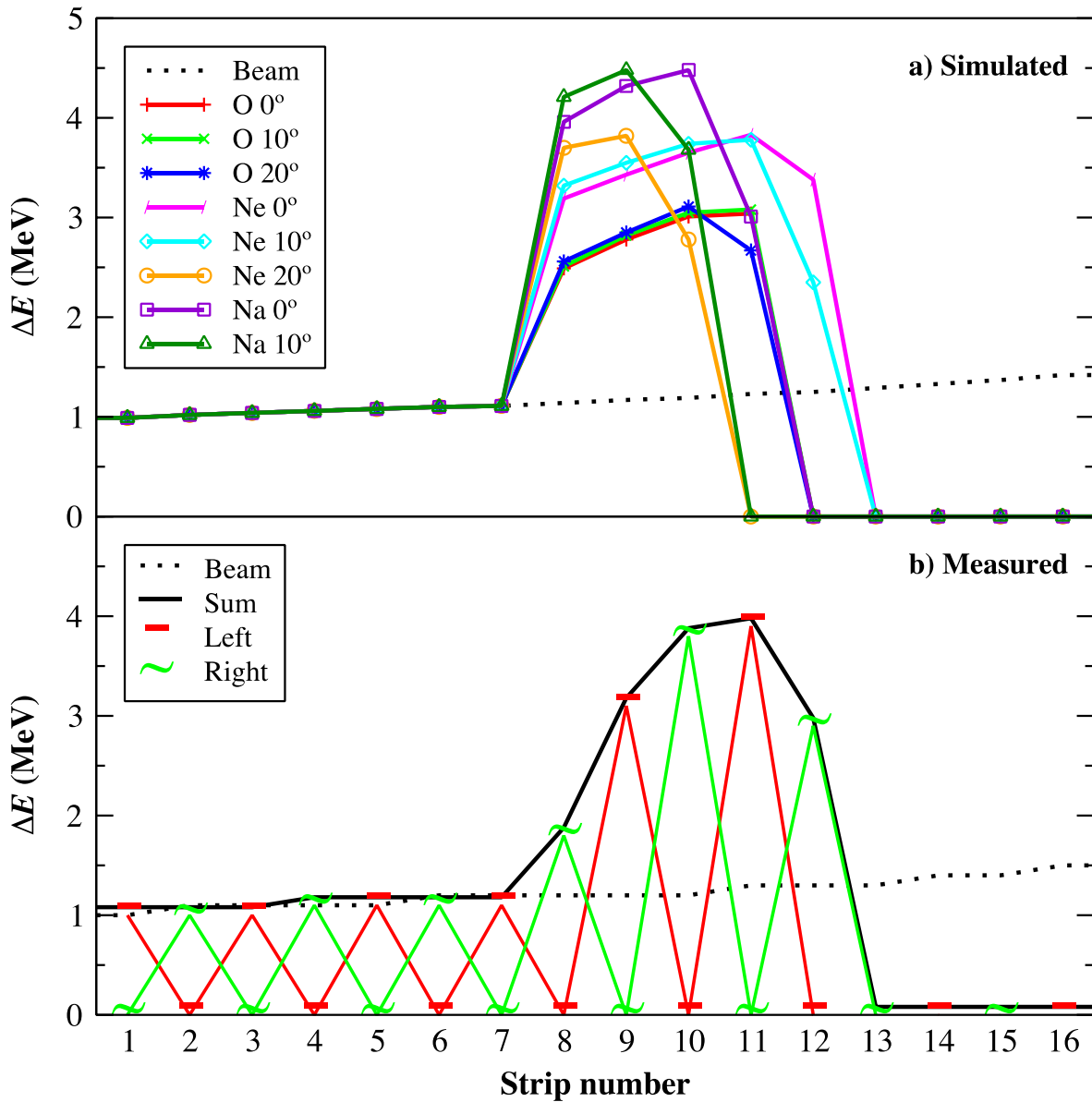
121 Since angular distributions of ERs from fusion reactions in this mass and energy range generally peak at
 122 0° in the laboratory frame and extend to scattering angles of about 35° (see e.g. Ref. [1]) practically the
 123 full yield of the fusion reactions can be detected in the first 10-12 strips. Fusion events occurring in the
 124 last 4-6 strips will experience some losses in efficiency.



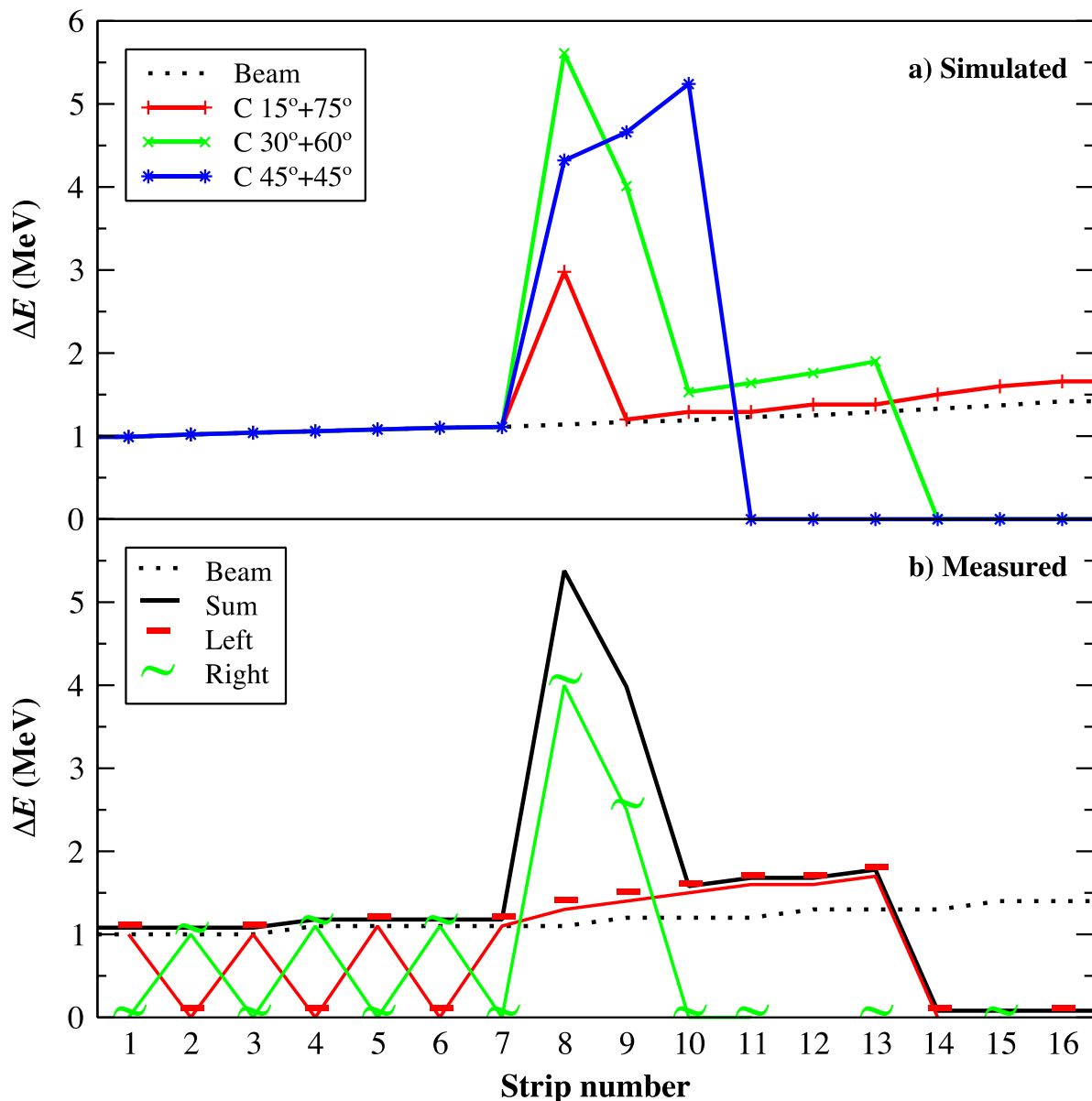
125
 126 Fig. 2 (color online). Experimental traces measured with the MUSIC detector. Black lines correspond to beam
 127 particles interacting with the gas target only by ionization. The red lines correspond to fusion events occurring in
 128 strip number 3. Note the presence of the fusion features described in the text, meaning a jump in ΔE followed by
 129 zero pulse height in strips higher than 10.

131 The signals from anode strips 0 and 17, at the beginning and at the end of the ionization chamber, are
 132 used for particle identification (see Sect. 3.3) or as veto signals to eliminate events occurring in the
 133 entrance and exit windows.

134 Another advantage of the multi-sampling method is that the fusion measurement is self-normalizing, since
 135 the beam and the fusion events at the various energies are obtained by the same detector using the same
 136 number of incident particles without the need to change the energy or using a monitor detector.



137
 138 Fig. 3 (color online). Comparison between simulated and experimental fusion signals occurring in strip number 8: a)
 139 fusion events simulated with FLUKA, b) left- and right-side signals for a measured fusion event. The “zigzag”
 140 structure in the left (red) and right (green) signals is the main feature of a multiplicity-one event.



142

143 Fig. 4 (color online). Simulated and experimental traces for scattering events occurring in strip number 8: a)
 144 scattering events simulated with FLUKA, b) a scattering event measured with the MUSIC detector. The simulated
 145 signals in a) correspond to two carbon nuclei scattered at angles that add up to approximately 90° ($15^\circ+75^\circ$, $30^\circ+60^\circ$
 146 and $45^\circ+45^\circ$). In b), note that after the beam-like pattern, there are signals in both sides of the same strip. This is an
 147 example of a multiplicity-two event.

148 In order to eliminate elastic or inelastic scattering events, which might interfere with fusion events, the
 149 anode strips 1–16 are subdivided into two staggered sections (marked “L” and “R” in the lower panels of
 150 Figs. 1 and 2). The two sections are used as a multiplicity filter. Since light particles (such as p, α)
 151 evaporated by the compound nucleus generate signals that are below the detection threshold, fusion
 152 events have multiplicity one (i.e., signals that occur either in the right or in the left side of the anode

153 strips). Elastic and inelastic scattering events on the other hand have two particles in the outgoing channel
154 producing events that can be rejected using the “beam-right” and “beam-left” information.

155 The response of the MUSIC detector to various reaction types was simulated using the Monte Carlo code
156 FLUKA [17]. Results from the simulation of a 45 MeV ^{13}C beam interacting with CH_4 are presented in
157 Figs. 3 and 4. Figure 3 shows simulated (a) and experimental (b) traces of fusion (multiplicity-one)
158 events. Fusion events have a pulse height that is typically a factor of 3-4 higher than the pulse height
159 produced by a beam-like particle. Although the FLUKA simulation gives an indication of a grouping of
160 the pulse height according to the nuclear charge of the ERs, variations of the emission angle and of the
161 location of the fusion reaction in a strip smear out this grouping. Simulated traces of events originating
162 from elastic/inelastic scattering at a few scattering angles are shown in Fig. 4a. Since for scattering of
163 same-mass particles the relative angle of the two particles is approximately 90° in the laboratory system,
164 events from e.g. $\pm 45^\circ$ or $+75^\circ$ and -15° need to be summed as shown in Fig. 4a. These events also show a
165 jump in the trace as observed for fusion, but as shown in Fig. 4b they produce signals on both sides of the
166 same strip.

167

168 3. Experimental details

169 3.1. Ionization chamber

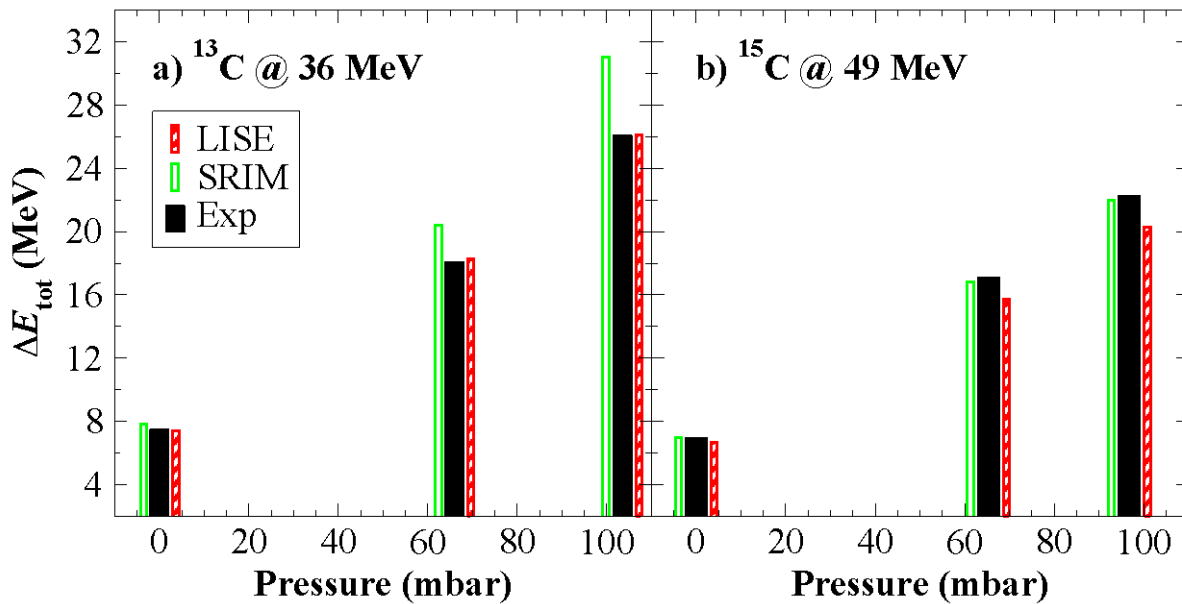
170 For the experiments described in this paper, the MUSIC detector was filled with methane gas at a pressure
171 of 200 mbar. Methane is a fast counting gas with drift velocities up to $10\text{ cm}/\mu\text{s}$ [18]. The electric field to
172 pressure (\mathcal{E}/p) ratios in the MUSIC detector were between 0.5 to $1\text{ V}/(\text{cm mbar})$. The gas pressure in the
173 ionization chamber was controlled by a pressure-regulated gas handling system. This gas handling system
174 has a high precision pressure gauge and magnetic valves which, together with a vacuum pump, establish a
175 constant flow of the counting gas. In this way, the pressure is maintained at a fixed preset value
176 preventing the detector/target gas from degradation. The pressure gauge of the gas-handling system was
177 calibrated against a high-precision Wallace & Tiernan gauge [19]. The gas temperature was also
178 monitored in order to obtain the density needed for calculating the cross sections. The energy deposited in
179 the detector by an incident beam-intensity of approximately 10^4 particles/s corresponds to a heat load of
180 less than $1\text{ }\mu\text{J}$, which is too low to cause a change in temperature.

181 The correct identification of fusion events with the MUSIC detector requires that only one incoming
182 particle is inside each “beam bucket”. While this is usually not a problem for secondary beams that
183 experience a reduction in intensity by a factor of 10^{5-6} relative to the primary beam incident on the
184 production target, for stable beams the intensity needs to be reduced accordingly. In order to avoid pile-up
185 in the IC, which has typical electron drift times of 1-2 μs , we used the RF beam-sweeper at ATLAS. This
186 device was operated as a chopper and increased the time between two consecutive beam bunches from 82
187 ns to 4-10 μs .

188

189 3.2. Energy measurement

190 For obtaining an excitation function, an energy value must be associated to each strip. Normally this is
 191 done by using energy-loss tables from the literature (e.g. LISE++ [20], SRIM [21]). It is also known,
 192 however, that these tables differ in their predictive power by up to 10% [21]. In order to measure the
 193 correct energy loss, MUSIC was mounted in front of the Enge-Split-Pole spectrograph (SPS) that was
 194 calibrated with α particles from a ^{228}Th source. Beams of $^{13,15}\text{C}$ were passing through the MUSIC detector
 195 filled with CH_4 at various pressures. The experimental energy loss values measured in the spectrograph
 196 are shown as the solid bars in Fig. 5, compared to the predictions of the codes LISE++ (v. 9.7) and SRIM
 197 (v. 2013). For a ^{13}C beam the LISE++ parameterization shows the best agreement, while for ^{15}C SRIM
 198 gives a slightly better overlap with the data. We used the LISE++ values for those cases where no
 199 spectrograph calibration has been performed. From these (calculated) energy losses, the energy value
 200 corresponding to each strip is obtained taking into account their finite size and assuming that fusion
 201 occurs in the middle of the strip.



202

203 Fig. 5 (color online). Comparison between calculated (LISE++ 9.7, SRIM 2013) and experimental total energy
 204 losses in the MUSIC detector, as a function of the gas pressure.

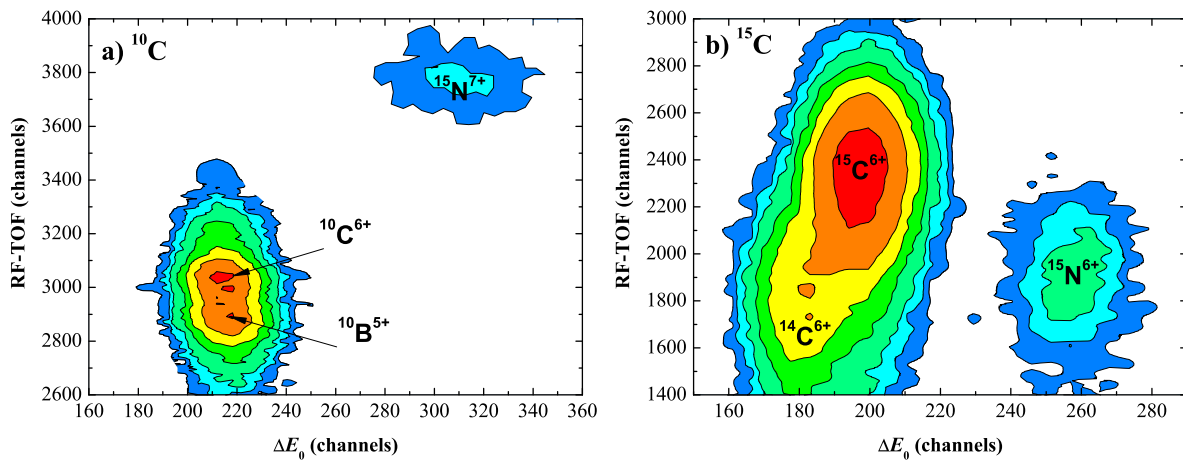
205

206 3.3. Particle identification in experiments with secondary beams

207 At the present radioactive beam facilities, the secondary beams have typically contaminants of various
 208 sorts. Therefore, it is necessary to tag each incoming particle according to its mass and Z number. At
 209 ATLAS, the beam is pulsed with a period of 82 ns. The measurement of the time of arrival of the beam
 210 particle in the IC with respect to the RF signal from the accelerator allows us to identify the various
 211 particle groups obtained in the production of secondary beams [15].

212 Examples of beam contaminants of radioactive beams produced via the inverse (p,n) or (d,p) reactions
 213 can be found in the literature [15, 22]. In this paper we briefly describe two examples of the particle

214 identification procedure. The ^{10}C beam was produced with the in-flight technique via the $^1\text{H}(^{10}\text{B},^{10}\text{C})\text{n}$
 215 reaction by bombarding a hydrogen-filled gas cell with an 80 MeV $^{10}\text{B}^{4+}$ beam from the ATLAS
 216 accelerator. The main contaminant observed in this case came from the primary ^{10}B beam which could be
 217 suppressed using time-of-flight and energy loss signals in the control strip S_0 of the ionization chamber
 218 (see Fig. 6a). The other contaminant was $^{15}\text{N}^{6+}$ from the ECR ion source and was well separated from ^{10}C .
 219 The ^{15}C beam was produced via the $\text{d}(^{14}\text{C},^{15}\text{C})\text{p}$ reaction by bombarding a deuterium-filled gas cell with a
 220 ^{14}C beam from the tandem accelerator at ATLAS, using a ^{14}C sputter target in the negative ion source.
 221 Since nitrogen does not form negative ions a pure ^{14}C beam is injected into the accelerator. The beam
 222 contaminants in this case included ^{14}C from the production beam as well as ^{15}N particles produced via the
 223 $\text{d}(^{14}\text{C},^{15}\text{N})\text{n}$ reaction. Again a measurement of the time of arrival of the beam bunches at MUSIC together
 224 with the energy loss in the control strip S_0 allowed a separation of the particles of interest from the
 225 contaminants as shown in Fig. 6b.



226

227 Fig. 6 (color online). ΔE_0 vs. RF-ToF spectra showing the separation between the secondary beams and the
 228 contaminants generated by the primary beams for a) 43 MeV ^{10}C and b) 49 MeV ^{15}C secondary beams.

229

230 4. Experimental Results

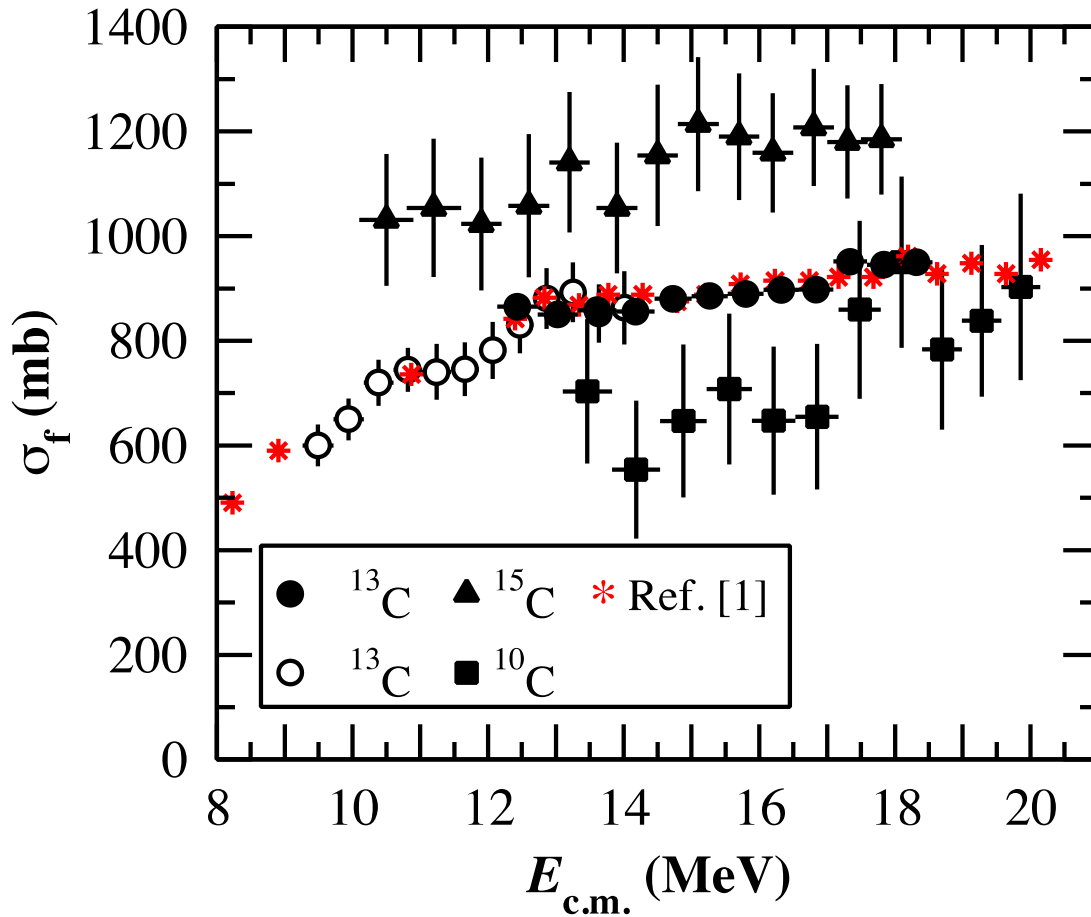
231 In order to demonstrate the capabilities of the MUSIC technique we discuss the experimental results of
 232 the $^{13}\text{C}+^{12}\text{C}$ and $^{10,15}\text{C}+^{12}\text{C}$ fusion reactions using a stable ^{13}C and secondary $^{10,15}\text{C}$ beams. The main
 233 experimental parameters are summarized in Table 1.

234 The analysis of the signals from the MUSIC detector was performed on an event-by-event basis. The
 235 analysis consisted of counting the number of beam-like particles needed for normalization and of the
 236 fusion events identified by their large energy loss, their length (typically covering 3-5 strips) and the lack
 237 of energy-loss signals in the strips further downstream (see Sect. 2). Due to those requirements, the
 238 detector provided only 11-13 data points. The effective target thickness needed for the cross section was
 239 derived from the width of the individual anode strips and the pressure and the temperature of the CH_4 gas
 240 in the detector.

241 Table 1. Main parameters of the MUSIC experiments: beam isotope, incident beam energy, ionization gas pressure,
 242 and center of mass energy range for the $^{A}\text{C}+^{12}\text{C}$ system measured in strips 1-16.

Beam	E_{lab} (MeV)	Pressure (mbar)	$E_{\text{c.m.}}$ range (MeV)
^{13}C	36	200	7.6 - 14.0
	45	200	9.9 - 18.3
^{10}C	43	240	9.5 - 19.9
^{15}C	49	200	8.9 - 18.3

243



244

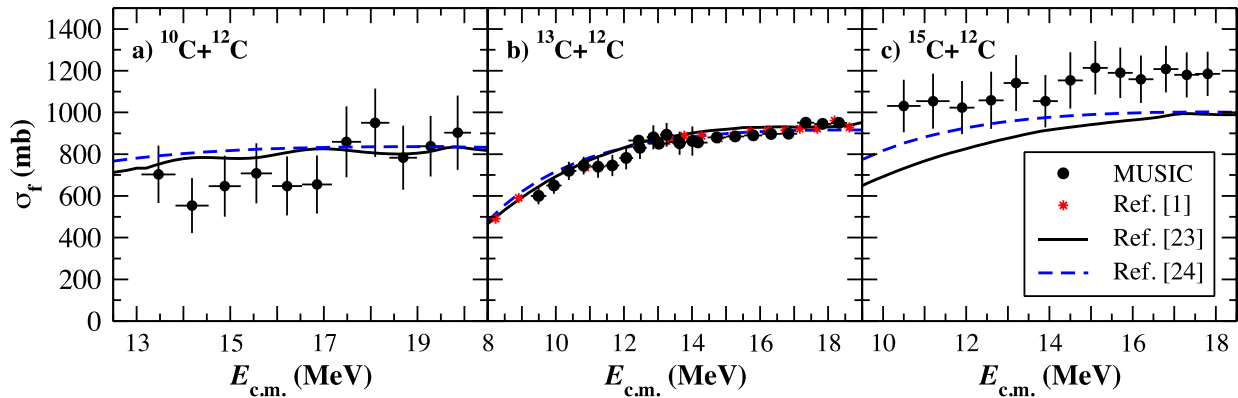
245 Fig. 7 (color online). Experimental $^{10,13,15}\text{C}+^{12}\text{C}$ fusion excitation functions from the present work. For the $^{13}\text{C}+^{12}\text{C}$
 246 case two different incident energies were used (open circles correspond to 36 MeV and filled circles correspond to
 247 45 MeV). The experimental data from Ref. [1] for the $^{13}\text{C}+^{12}\text{C}$ system are also included for comparison.

248 Since precise measurements of these parameters were obtained, the overall uncertainty in the cross
 249 sections is determined by the statistics of the experiment.

250 The uncertainty in the energy values of the excitation function originates from the finite size of the strips
 251 since fusion can occur at different positions, and hence with different energies, in the same strip. For this
 252 reason, we report the energy uncertainty as the calculated energy loss in each strip. For the current
 253 experiments it varied between 2% and 6% of the c.m. energy, increasing with strip number.

254 The fusion cross sections measured for the systems $^{10,13,15}\text{C}+^{12}\text{C}$ are shown in Fig. 7. For the $^{13}\text{C}+^{12}\text{C}$ case
 255 two measurements with different incident beam energies (36 and 45 MeV), but the same gas pressure,
 256 were performed (see Table 1). The intention of these first test measurements was to study the operation of
 257 the detector and the consistency of the analysis process with a set of overlapping excitation functions for a
 258 system that has been measured using one of the standard techniques. The results are compared to the data
 259 from Ref. [1] in Fig. 7b and an excellent agreement is observed.

260 The data corresponding to $^{10,15}\text{C}+^{12}\text{C}$ are the first fusion measurements obtained for these systems. The
 261 shapes of the excitation functions are all similar, with a plateau at the higher energies and a fall-off of the
 262 cross sections towards lower energies. Because of the limited statistics achieved with radioactive beams,
 263 the uncertainties in σ_f for $^{10,15}\text{C}+^{12}\text{C}$ are higher than for the stable-beam reaction $^{13}\text{C}+^{12}\text{C}$, reaching about
 264 12% in the former case.



265
 266 Fig. 8 (color online). Comparison of MUSIC experimental data with theoretical calculations. Solid circles:
 267 experimental data obtained with the MUSIC detector. Solid lines: theoretical cross sections from coupled-channels
 268 calculations [23]. Dashed lines: predictions from a barrier penetration model using the São Paulo potential [24].

269 In Fig. 8 we have compared the measured cross sections with various theoretical predictions. The solid
 270 lines are the predictions from coupled-channels calculations. These calculations were done using a
 271 double-folding potential and including couplings to one- and two-phonon excitations as well as mutual
 272 quadrupole and octupole excitations in projectile and target [23]. The dashed lines are the results of a
 273 barrier-penetration model based on the São Paulo potential [24] (previously shown as astrophysical S-
 274 factors in Ref. [25]). In the $^{13}\text{C}+^{12}\text{C}$ case (Fig. 8b), the agreement between both models and the
 275 experimental data is excellent. On the other hand, in the radioactive beam cases, the São Paulo potential
 276 predictions are about 10% above the coupled-channels results. The two models overestimate the

277 experimental data for $^{10}\text{C}+^{12}\text{C}$ in the $E_{\text{c.m.}} = 13\text{-}17$ MeV energy range and show better agreement at higher
278 energies. Both models underestimate the experimental cross sections in the $^{15}\text{C}+^{12}\text{C}$ case.

279

280 **5. Summary**

281 We have developed and tested a new high-efficiency, active-target system in the form of a small multi-
282 sampling ionization chamber. This detector allowed us to determine a large part of the excitation function
283 in a single measurement, thus saving considerable running time and eliminating difficulties with the
284 relative normalization of the cross sections. Since the detector operates at low beam intensities, it is
285 ideally suited for experiments with the radioactive ion beams that are available at present-day facilities.
286 The separation of beam contaminants in experiments with these beams was achieved by measuring the
287 energy loss and the time-of-flight of the secondary radioactive beam particles.

288 The performance of the MUSIC detector was tested in experiments with stable ^{13}C and radioactive $^{10,15}\text{C}$
289 beams. The agreement with data from the literature for the ^{13}C case was excellent. Monte Carlo
290 simulations using the code FLUKA were used to understand how to correctly identify the various nuclear
291 processes and to develop an algorithm to extract the fusion cross sections. In this way, we obtained a full
292 characterization of the detector that we can use to predict its response in future experiments.

293 The main disadvantage of the MUSIC detector in its present form is the relatively low beam rate it can
294 tolerate in order to avoid pile-up effects that could be interpreted as fusion events. At a pulsed beam
295 accelerator such as ATLAS, this is achieved by having at most one particle in each bunch and separating
296 the bunches with a sweeper system. In this way, the beam bunches arrive to the detector at intervals of
297 about $5\ \mu\text{s}$, which is the typical drift time in the ionization chamber. Improving the count rate capability
298 of the MUSIC detector by introducing a “gating” grid [26, 27] is planned in the future. Other upgrades
299 include the addition of parallel-plate-avalanche counters at the entrance and exit for better timing signals
300 and measurements of the vertical drift times.

301 In these first experiments we have demonstrated that the MUSIC detector is a powerful device especially
302 for the measurement of fusion reactions with radioactive beams. Measurements involving other
303 isotopically pure gases (He, Ne, Ar) have already started.

304

305 **Acknowledgments**

306 We thank the operations crew of the ATLAS accelerator for providing the beams used in these
307 experiments. This work was supported by the US Department of Energy, Office of Nuclear Physics under
308 contract No. DE-AC02-06CH11357, and the Consejo Nacional de Investigaciones Científicas y Técnicas
309 (CONICET), Argentina.

310

311 **References**

- 312 [1] D. G. Kovar et al., Phys. Rev. C **20**, 1305 (1979).
- 313 [2] X. D. Tang et al., J. Phys.: Conf. Ser. **381**, 012120 (2012).
- 314 [3] B. Dasmahapatra et al., Nucl. Phys. A **565**, 657-670 (1993).
- 315 [4] R. A. Dayras et al., Nucl. Phys. A **265**, 153 (1975).
- 316 [5] T. Spillane et al., Phys. Rev. Lett. **98**, 122501 (2007).
- 317 [6] M. Notani et al., Nucl. Phys. A **834**, 192 (2010).
- 318 [7] D. Di Gregorio et al., Phys. Lett. B **176**, 322 (1986).
- 319 [8] J. O. Fernández Niello et al., Phys. Rev. C **43**, 2303 (1991).
- 320 [9] A. J. Pacheco et al., Comp. Phys. Comm. **52**, 93-102 (1988).
- 321 [10] M. Alcorta et al., Phys. Rev. Lett. **106**, 172701 (2011).
- 322 [11] K. E. Rehm et al., Nucl. Inst. Meth. A **344**, 614-622 (1994), and references therein.
- 323 [12] W. B. Christie et al., Nucl. Inst. Meth. A **255**, 466-476 (1987).
- 324 [13] K. Kimura et al., Nucl. Inst. Meth. A **297**, 190-198 (1990).
- 325 [14] Y. Mizoi et al., Nucl. Inst. Meth. A **431**, 112-122 (1999).
- 326 [15] B. Harss et al., Rev. Sci. Instr. **71**, 380-387 (2000).
- 327 [16] Mesytec GmbH & Co., <http://www.mesytec.com/nuclear.htm>.
- 328 [17] G. Battistoni et al., AIP Conf. Proc. **896**, 31-49 (2007).
- 329 [18] Th. Berghoefter et al., Nucl. Inst. Meth. A **525**, 544-552 (2004).
- 330 [19] FLW Inc., <http://www.wallaceandtiernan-usa.com/absolute-pressure-gauges-1500-8A.html>.
- 331 [20] O. B. Tarasov and D. Bazin, Nucl. Instr. Meth. B **266**, 4657-4664 (2008). <http://lise.nscl.msu.edu>.
- 332 [21] J. F. Ziegler et al., Nucl. Inst. Meth. B **268**, 1818-1823 (2010). <http://www.srim.org>.
- 333 [22] X. D. Tang et al., Phys. Rev. C **81**, 045809 (2010).
- 334 [23] H. Esbensen et al., Phys. Rev. C **84**, 064613 (2011), and private communication.
- 335 [24] D. G. Yakovlev et al., Phys. Rev. C **82**, 044609 (2010).
- 336 [25] P. F. F. Carnelli et al., Phys. Rev. Lett. **112**, 192701 (2014).
- 337 [26] P. Nemethy et al., Nucl. Inst. Meth. A **212**, 273-280 (1983).

338 [27] T. Hashimoto et al., Nucl. Inst. Meth. A **556**, 339-349 (2006).